Applied and Environmental Microbiology, July 2011, p. 4939–4948 Vol. 77, No. 14
0099-2240/11/$12.00 doi:10.1128/AEM.00407-11
Copyright © 2011, American Society for Microbiology. All Rights Reserved.

Impact of Internal RNA on Aggregation and Electrokinetics of Viruses: Comparison between MS2 Phage and Corresponding Virus-Like Particles[▽]

C. Dika,[1] J. F. L. Duval,[2]* H. M. Ly-Chatain,[1] C. Merlin,[1] and C. Gantzer[1]*

Laboratoire de Chimie Physique et Microbiologie pour l'Environnement, Nancy-Université, CNRS, Faculté de Pharmacie, 54000 Nancy, France,[1] and Laboratoire Environnement et Minéralurgie, Nancy-Université, CNRS, 54501 Vandoeuvre-lès-Nancy cedex, France[2]

Received 23 February 2011/Accepted 18 May 2011

We compare for the first time the electrokinetic and aggregation properties of MS2 phage (pH 2.5 to 7, 1 to 100 mM $NaNO_3$ electrolyte concentration) with those of the corresponding virus-like particles (VLPs), which lack entirely the inner viral RNA component. In line with our previous work (J. Langlet, F. Gaboriaud, C. Gantzer, and J. F. L. Duval, Biophys. J. 94:3293-3312, 2008), it is found that modifying the content of RNA within the virus leads to very distinct electrohydrodynamic and aggregation profiles for MS2 and MS2 VLPs. Under the given pH and concentration conditions, MS2 VLPs exhibit electrophoretic mobility larger in magnitude than that of MS2, and both have similar isoelectric point (IEP) values (~4). The electrokinetic results reflect a greater permeability of MS2 VLPs to electroosmotic flow, developed within/around these soft particles during their migration under the action of the applied electrical field. Results also support the presence of some remaining negatively charged component within the VLPs. In addition, MS2 phage systematically forms aggregates at pH values below the IEP, regardless of the magnitude of the solution ionic strength, whereas MS2 VLPs aggregate under the strict condition where the pH is relatively equal to the IEP at sufficiently low salt concentrations (<10 mM). It is argued that the stability of VLPs against aggregation and the differences between electrokinetics of MS2 and corresponding VLPs conform to recently developed formalisms for the stability and electrohydrodynamics of soft multilayered particles. The differences between the surface properties of these two kinds of particles reported here suggest that VLPs may not be appropriate for predicting the behavior of pathogenic viruses in aqueous media.

Understanding the behavior of virus particles of enteric pathogens (e.g., norovirus, hepatitis A virus) in terms of aggregation or adhesion is mandatory for addressing appropriately the processes involved in, e.g., viral dissemination or water treatment (9, 11). In that respect, much effort is now devoted to the analysis of the so-called surface properties of viruses, which are impacted by solution pH, ionic strength, or the presence of organic matter (20). The importance of viral surface properties within the framework of water treatment is well illustrated by the relationship between the efficiency of membrane filtration for removing viruses and the charge and degree of hydrophobicity of these biocolloids (11).

According to standard formulations of Derjaguin-Landau-Verwey-Overbeek (DLVO) representation and electrokinetic theories for hard (impermeable) particles, a parameter commonly used as an indicator for the sign and magnitude of charge carried by a virus in a solution of given pH is the difference between the pH and the so-called isoelectric point (IEP) of the virus, defined as the pH value at which virus electrophoretic mobility is zero (14). Within the regime of partial dissociation of charges located at the surface, the higher (or lower) the solution pH is than the IEP, the more negative (or positive, respectively) is the viral charge, and the reverse is true for a pH value lower than the IEP. Along this line of reasoning, MS2 phage is classically viewed as a model system for defining the performance of membrane or sand filtrations with respect to removal of pathogenic viruses. One reason for this is the low IEP of MS2 phage (about 3.5), which corresponds to the (supposedly) worst possible situation (20, 25) in terms of (repulsive) electrostatic interactions between the virus and the membrane and thus membrane removal efficiency in aqueous media at neutral pH. Note that this use of MS2 as a model system (25, 27) has been adopted despite the limited knowledge on the surface properties of pathogenic viruses, such as noroviruses. A major difficulty for studying noroviruses is that they are nonculturable and therefore cannot be produced in sufficiently high concentration for appropriate physicochemical analysis. As a result, one alternative apart from considering MS2 as a model system consists of the use of synthetic viral particles known as virus-like particles (VLPs). Usually, VLPs are produced after the structural genes of a given virus capsid protein are expressed and then self-assemble to form a supposedly empty (virus-like) particle. The first norovirus VLPs were produced for the Norwalk virus in 1992, and this initiated the use of these particles as model systems (7) for understanding and predicting the behavior of viruses in filtration processes (17, 21) or in terms of persistence in shellfish

* Corresponding author. Mailing address for C. Gantzer: Laboratoire de Chimie Physique et Microbiologie pour l'Environnement, Nancy-Université, CNRS, 5 Rue Albert Lebrun, F-54250 Nancy, France. Phone: 33 3 83 68 22 91. Fax: 33 3 83 68 23 78. E-mail: Christophe.Gantzer@pharma.uhp-nancy.fr. Mailing address for J. F. L. Duval: Laboratoire Environnement et Minéralurgie, Nancy-Université, CNRS, 15 Avenue du Charmois, 54501 Vandoeuvre-Lès-Nancy, France. Phone: 33 3 83 59 62 63. Fax: 33 3 83 59 62 55. E-mail: Jerome.Duval@ensg.inpl-nancy.fr.

▽ Published ahead of print on 27 May 2011.

Sarepta Exhibit 1035, page 1

Downloaded from https://journals.asm.org/journal/aem on 18 December 2024 by 72.80.70.191.

(13). Norovirus VLPs are morphologically and antigenically similar to the viruses from which they are derived, except that they are lacking the viral genome and therefore are not pathogenic. Both types of particles were shown to exhibit similar stability features regarding their integrity with respect to pH and temperature conditions (1a).

While IEP data surely contribute to addressing the overall charge/surface properties of viruses as a function of pH, it must be recognized that they only partly reflect the electrostatic properties of these particles. The IEP value of viruses, which are paradigms of permeable (soft) multilayered biocells (10), is significantly impacted by their permeability to external flow (electroosmotic flow developed during the migration of the particles under the action of the externally applied field), as theoretically and experimentally demonstrated by Langlet et al. (10). The IEP of soft multilayered particles is generally a complex, ionic-strength-dependent signature of the intertwined electrostatic and permeability properties of the whole particle. Contrary to common belief, the IEP does not depend solely on the nature of the viral surface charge (in particular, pK value), i.e., the charge located at the outer edge of the capsid part of the virus. Instead, it is governed by the respective physicochemical characteristics (e.g., nature and spatial distribution of charges, permeability) of the layers constituting the particle, i.e., the inner RNA and the outer proteic capsid in the case of F-specific RNA bacteriophages (e.g., MS2) and noroviruses.

For MS2 phage, the measured IEP value (~3.5 to 3.9) is lower than that expected if considering the capsid (IEP of >8) (10, 15, 19) only. As detailed previously (10), the dependence of electrophoretic mobility of MS2 phage on solution ionic strength is typical of that classically encountered for soft (i.e., permeable) particles. In particular, the interpretation of data according to rigorous theory for multilayered soft-particle systems (like MS2) evidenced that permeability of MS2 to electroosmotic flow allows a significant intrusion of flow within the inner RNA component. In turn, IEP value and MS2 mobility are significantly impacted by particle permeability and nature of the charges (e.g., number density and pK dissociation values) located within the heart of the virus. Then, the measured electrophoretic mobility significantly reflects the chemical composition of the virus genome, for which the zero point of charge is about 2.9 (10). This dismisses the interpretation of the low IEP value given by Penrod et al. (15), who argued that the IEP value and thereby the virus mobility reflect the sole contribution of the amino acids located at the outer edge of the capsid. Such line of reasoning is indeed incompatible with the presence of a finite mobility plateau value (nonzero plateau value) at large ionic strengths. This plateau denotes a strong permeation of the virus to flow (see computations in reference 10) and therefore a strong contribution of internal RNA in defining the electrokinetics of MS2 as a whole. Such behavior is characteristic of permeable colloids, whereas a monotonous decrease of the mobility toward zero value is expected for hard (i.e., impermeable) biocolloidal systems (3, 4) under high-salinity conditions.

In line with these elements, much theoretical and experimental work now clearly evidences that electrophoretic mobility of soft bioparticles, like viruses or bacteria, cannot simply be converted into a zeta potential or interpreted in terms of surface charge (3). Instead, to achieve a quantitative interpretation of the electrokinetic response of viruses, a rigorous evaluation of the fundamental electrohydrodynamic equations must be carried out, taking into account the variations in soft-material density, chemical composition, and degree of flow penetration from the center of the virus (RNA part) to the outer peripheral shell layer (capsid part) (10).

To the best of our knowledge, available reports in the literature on the physicochemical properties of noroviruses over a large range of ionic strengths and pH values are based on data collected for VLPs, which are viewed as surrogates. Because previous studies (9, 10, 11) suggested a significant role of the internal genome in governing the overall electrokinetic properties of (complete) viral particles, the question arises whether or not VLPs may truly be considered model systems for their pathogenic equivalents. In this study, we report the first comparison between a virus (in this case, MS2) and its corresponding VLPs in terms of electrokinetic and aggregation properties. Qualitative comparison of the electrophoretic mobilities, measured for these particles as a function of ionic strength and pH, gives insight into their respective electrostatic and flow permeability properties. Furthermore, size measurements were carried out to provide additional information on the stability of these viruses with respect to aggregation, recalling that stability is governed partly by the charge properties of the virus. Major differences are found for the two types of viral particles examined. This means that VLPs may not be suitable model systems for predicting behavior of pathogenic viruses, mainly because of the significant impact of the internal genome on the overall physicochemical properties of viruses.

MATERIALS AND METHODS

Preparation of suspensions of MS2 F-specific RNA phage. MS2 bacteriophage was obtained from a reference culture (ATCC 15597-B1). The phage was replicated according to the procedure NF EN ISO 10705-1 (October 2001; 1) using *Escherichia coli* Hfr K-12 (ATCC 23631) as host cells. After replication, the suspension of phage was centrifuged (Beckman model J2-22, 27,000 × *g*, 60 min, 4°C), and the supernatant was filtered using a 0.22-μm membrane (Millex-GP; Millipore). The suspension was then purified by dialysis with a 100,000-molecular-weight cutoff (131420; Spectrum), first against deionized water for 14 h and then against $NaNO_3$ 1 mM, pH 6.7, for 14 h. In a final step, the phage suspension was filtered once more using a 0.22-μm membrane and stored in $NaNO_3$ 1 mM at 4°C prior to any measurement. The viral concentration obtained following the above-described protocol was ~3.10^{11} PFU ml^{-1}.

Synthesis of MS2 VLPs. The plasmid pETCT, containing the MS2 capsid gene cloned under the control of a T7 promoter, was kindly provided by D. S. Peabody (University of New Mexico) and introduced into strain BL21(DE3) of *E. coli* (12) using standard transformation procedures (18). MS2 VLPs were produced from strain BL21(DE3)(pETCT) according to the method of Lima et al. (12), with slight modifications. Briefly, *E. coli* BL21(DE3)(pETCT) was cultivated in LB (lysogeny broth) supplemented with 50 μg ml^{-1} ampicillin (pETCT selection) at 37°C. At an optical density at 600 nm (OD_{600}) of 0.6, the culture was induced for the production of the capsid protein with 1 mM IPTG (isopropyl-β-D-thiogalactopyranoside) for 3 h at 37°C. Cells were then collected by centrifugation (6,000 × *g*, 20 min, 4°C), resuspended in a 1 mM solution of $NaNO_3$ at pH 8 (1/5 of the initial volume), and further treated with 0.05 mg ml^{-1} of lysozyme for 30 min at room temperature, after which they were finally sonicated for 3 min at 51 W. Cell debris was eliminated by centrifugation (13,500 × *g*, 20 min, 4°C), and the VLP-containing supernatant was filtered through a 0.22-μm membrane (Millex-GP) before storage at 4°C. Proteins from the collected capsid were analyzed both by SDS-PAGE with Coomassie blue staining and by transmission electronic microscopy to further ascertain the self-assembly of the proteins as VLPs and their "empty" character (Fig. 1D). SDS-PAGE results obtained for both MS2 and VLPs revealed the same bands, including that corresponding to the coat protein (14,000 Da). However, the absence of maturase in the proteic capsid of

Downloaded from https://journals.asm.org/journal/aem on 18 December 2024 by 72.80.70.191.

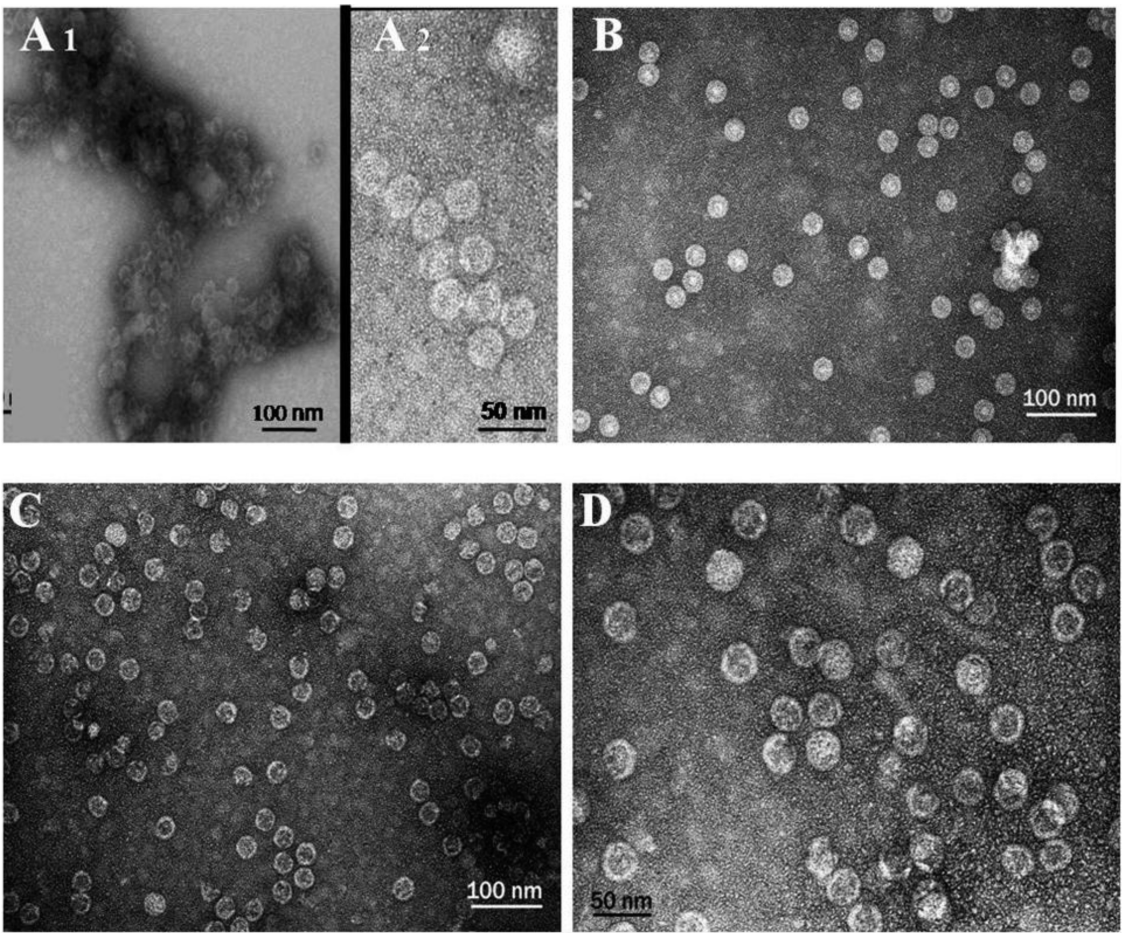

FIG. 1. Transmission electron microscopy of MS2 bacteriophage (A and B) and MS2 VLPs (C and D) at pH 3 (A and C) and pH 7 (B and D). MS2 phage and VLPs initially obtained in $NaNO_3$ 1 mM solution were adsorbed on the grids and negatively stained with uranyl acetate. Samples were observed with magnifications of ×50,000 (bar, 100 nm) and ×80,000 (bar, 50 nm).

VLPs cannot be demonstrated because its concentration is 180 times lower than that of the major capsid proteins.

Transmission electron microscopy. The samples of interest in this study were adsorbed on grids and negatively stained with 2% uranyl acetate. Then, they were examined at 200 kV and magnifications of ×80,000 and ×50,000 using a Philips CM20 electronic microscope.

Size and electrophoretic mobility measurements. Prior to size and electrophoretic mobility measurements, MS2 and MS2 VLPs were filtered to eliminate possible large aggregates (0.22 μm). The sensitivity of the apparatus requires working with high viral suspension concentrations (up to 10^9 PFU ml^{-1}). Samples were then poured into a polypropylene tube directly screwed into a personal computer (PC)-monitored titrator connected to a Zetasizer NanoZS instrument. Size and electrophoretic mobility were measured as a function of pH (range of 2.5 to 7) in $NaNO_3$ electrolyte (concentration in the range of 1 to 100 mM) at 22 ± 0.1°C using a Zetasizer NanoZS instrument (He-Ne red laser, wavelength of 633 nm; Malvern Instruments, Malvern, United Kingdom). Experiments were driven by Dispersion Technology Software (DTS), provided by Malvern Instruments. Electrophoretic mobilities were measured by laser Doppler electrophoresis, also known as phase analysis light scattering. The rate of change of the phase shift between the scattered light and a reference beam is correlated to the particle velocity and thus allows for evaluating the electrophoretic mobility. The size distribution of the viral suspensions under investigation was determined using dynamic light scattering (DLS), also incorporated in the ZetaSizer NanoZS instrument mentioned above. DLS allows the measurement of the Brownian motion of the particles, that is, the time dependence of the intensity fluctuations. The diffusion coefficient (D) of the viruses can be extracted from appropriate fitting of the autocorrelation function. As a first approximation, the diffusion coefficient can be converted into particle size using the Stokes-Einstein equation.

Investigation of the effects of pH and ionic strength on viral size and electrophoretic mobility was carried out using an Autotitrator MPT-2 (Malvern, United Kingdom). It enables automatic variation of pH and ionic strength upon addition of predefined volume increments of HCl 0.1 M and NaOH 0.1 M and volume increments of $NaNO_3$ 0.1 mM, 1 mM, or 500 mM (all solutions were filtered with a 0.22-μm membrane). For a given pH and salt concentration, size and electrophoretic measurements were realized three to four times to ensure the repeatability of the results.

RESULTS

MS2 and MS2 VLP size measurements. The stability properties of MS2 and MS2 VLPs with respect to aggregation were determined by size measurements under different conditions of pH (from 2.5 to 7) and ionic strength (1, 10, and 100 mM). From results shown in Fig. 2A, we conclude that MS2 phage is in nonaggregated form for pH values greater than 4, irrespective of the ionic strength level in solution. Under such conditions, the diameters of the particles vary between 20 and 30 nm, which is in agreement with the size reported for MS2 particles (22, 23, 24). The size of the MS2 particles as obtained by DLS is supported by independent electron microscopy measurements (Fig. 1B) that confirm the presence of isolated viral particles all over the grid of observation. Conversely, for pH

Downloaded from https://journals.asm.org/journal/aem on 18 December 2024 by 72.80.70.191.

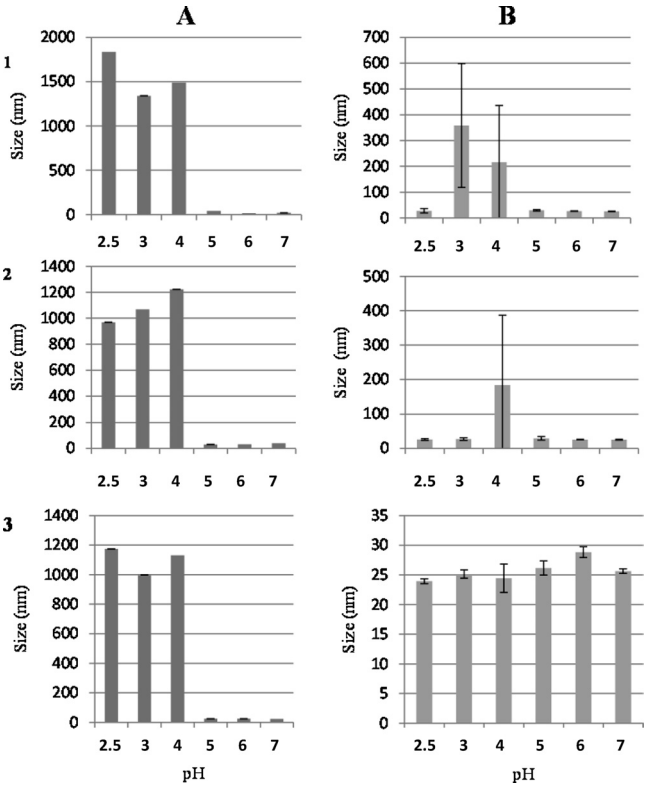

FIG. 2. Size (diameter) measurements for MS2 phage (A) and MS2 VLPs (B) as a function of pH (indicated) and $NaNO_3$ salt concentration (1 mM [1], 10 mM [2], and 100 mM [3]). Error bars indicate standard deviations.

values lower than or equal to 4, MS2 phage systematically forms aggregates over the entire range of salt concentrations examined. The mean effective size of these aggregates is between 1.2 μm and 1.8 μm. These results are in agreement with electron micrographs (Fig. 1A1) which clearly depict assemblies of viruses in contact with each other all over the grid. Magnification of these particle assemblies (Fig. 1A2) further suggests that the viral particles maintain their native structure within the aggregates.

Figure 2B displays the size measured for the VLPs as a function of pH and ionic strength. Clearly, the stability of MS2 VLP suspensions against aggregation dramatically differs from that of MS2 phage. Aggregation is detected for pH of ~3 to 4 at low electrolyte concentrations (1 mM and 10 mM), while suspensions of VLPs are stable against aggregation at 100 mM over the entire range of pH values tested. Aggregates of VLPs, when present, exhibit a mean size of about 200 to 300 nm, i.e., smaller than that obtained for MS2 aggregates at low pH. Keeping in mind the presence of MS2 VLP aggregates in a narrow pH window, electron microscopy reveals isolated MS2 VLPs at pH 3 and 7 in 1 mM $NaNO_3$ (Fig. 1C and D). The absence of aggregates at pH 3 from electron microscopy analysis seems to contradict the size measurements reported in Fig. 2B and obtained independently using NanoZS equipment. This discrepancy might be explained by the high instability of the VLP suspensions within a narrow pH window, so that, in turn, only small differences in pH from one VLP suspension to another may lead to the observation or lack of observation of VLP aggregates. This explanation is supported by the recent analysis by da Silva et al. (2) on the adsorption/aggregation properties of norovirus genogroup I and II (GI and GII) VLPs. These authors indeed argued that the "observed variability in [sticking coefficient] near the pI [i.e., isoelectric point] may be due to small differences in bulk pH that cause dramatic shift in charge balance."

All data discussed above were obtained in an experimental setup with continuous decreases in the pH and with the measurements of particle size carried out for a selection of pH values as shown in Fig. 2. This tends to demonstrate that MS2 VLP aggregation is a reversible phenomenon when the pH is gradually decreased below 3 to 4, which is not the case for MS2 phage. In order to rule out the possibility that MS2 aggregates obtained at pH 4 were in an irreversible state when the pH was further decreased, aggregation experiments were repeated in batches at pH values set independently. Here again, MS2 aggregation was systematically observed for pH values below 4. This suggests that, under such pH conditions, attractive forces associated with MS2 phage are dominant over repulsive forces.

Electrokinetics. The above-described aggregation profiles clearly point out basic differences regarding MS2 and MS2 VLP surface particles. Such differences in behavior were further investigated by electrokinetics. The electrophoretic mobilities (here denoted as μ) for MS2 phage and VLPs were measured as a function of pH in $NaNO_3$ solutions of concentration 1 mM, 10 mM, and 100 mM (Fig. 3). As a general comment, for a given salt concentration, the absolute value of the mobility ($|\mu|$) decreases when the solution pH is decreased and eventually changes sign at sufficiently low pH, as observed for VLPs. In addition, for both VLPs and MS2, $|\mu|$ decreases upon increase of salt concentration at fixed pH, in agreement with an increased screening of the particle charges by ions present in the medium (3, 10). However, the profiles of μ versus pH are significantly different for MS2 phage and corresponding VLPs. The striking feature is that μ measured for VLPs changes sign at pH values less than 3 to 4, while for MS2 phage, μ basically remains negative over the entire range of pH values. As noted in the Discussion, this basic difference in electrokinetic response of MS2 and MS2 VLPs coincides with the different stability properties of these particles against aggregation (Fig. 2). Langlet et al. (10) indeed demonstrated that predictions of soft-particle electrokinetic theory failed to recover mobility data of MS2 phage at lower pH values. Theoretical electrophoretic mobilities were systematically larger than experimental data and underpinned a clear change of sign in mobility, unobserved in experiments for MS2. The reason for the above-described discrepancy is that the theory outlined in reference 10 is valid strictly for isolated particles and is not applicable for aggregates, around/within which electroosmotic flow stream lines significantly differ from situations seen with isolated particles. Unlike MS2, VLPs do not aggregate at low pH, which is consistent with a clear change of sign for the electrophoretic mobility. The variation of μ with pH for VLPs roughly follows a sigmoid curve, reminiscent of that typically obtained for particles whose charge stems from the dissociation of amphoteric groups. Quantitatively, for a given salt concentration, $|\mu|$ measured at a pH of ~7 for VLPs is larger than that for MS2 phage under similar pH and ionic strength con-

Downloaded from https://journals.asm.org/journal/aem on 18 December 2024 by 72.80.70.191.

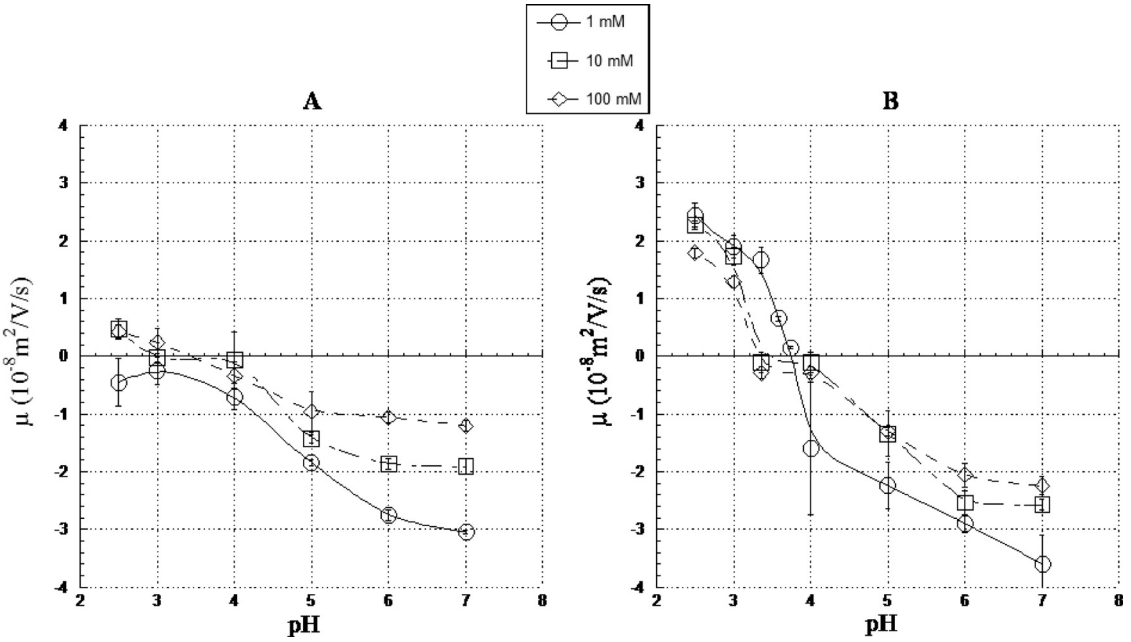

FIG. 3. Electrophoretic mobility of MS2 bacteriophage (A) and MS2 VLPs (B) as a function of pH for three $NaNO_3$ electrolyte concentrations, 1 mM, 10 mM, and 100 mM (indicated). The solid and dotted lines are only guides to the eye. Measurements were done in triplicate. Error bars indicate standard deviations.

ditions. When the pH is decreased, the rate of decrease for $|\mu|$ is higher for VLPs than for MS2 phage. From the data shown in Fig. 3, we obtain an IEP of about 3.4 to 3.8 for the VLPs, while that for MS2 is around 3.5, a value obtained by extrapolating to low pH the mobility measured for the nonaggregated form of MS2 at high pH.

The dependence of μ on salt concentration is shown in Fig. 4 for VLPs and MS2 under pH conditions where both types of particles are stable against aggregation (pH = 7). In the inset, mobility data are plotted according to a linear scale of salt concentration. As previously mentioned, $|\mu|$ decreases with increasing salt concentration as a result of particle charge screening. At sufficiently high concentrations, $|\mu|$ reaches asymptotically a nonzero plateau value. The presence of this plateau is typical for the soft (permeable) nature of the particles investigated, thereby confirming the inadequacy of converting mobility data into zeta potential or surface charge (3, 4). At a given electrolyte concentration, $|\mu|$ of VLPs is systematically larger than that of MS2. In addition, the rate of decrease of $|\mu|$ with increasing salt concentration is higher for MS2 than for VLPs. As extensively noted in the Discussion, the theory reported in reference 10 for electrokinetics of soft multilayered particles, like viruses, fully supports these experimental findings (Fig. 5).

DISCUSSION

From their analysis of electrokinetics of MS2 phage, Langlet et al. (10) concluded that MS2 phage is a paradigm of multilayered soft (or permeable) particles with the inner RNA and the outer proteic capsid as components, both permeable to external fluid flow as experienced by the virus in electrophoresis. The main purpose of the current study is to refine our understanding of the impact of the viral genome on the physicochemical properties of the virus, which are known to affect virus behavior under environmental conditions or the capacity for virus removal during water treatment. To do so, electrophoretic mobilities and particle sizes were compared for MS2 and corresponding VLPs as a function of pH and salt concentration.

MS2 phage and mobility data in literature. Penrod et al. (14) measured the electrophoretic mobility (μ) of MS2 in the pH range of 3 to 9 at a 10 mM NaCl concentration. Their results indicated that μ is independent of pH for pH values greater than 5, with a μ value of $\sim -0.7 \times 10^{-8}$ m^2 V^{-1} s^{-1}. The mobility further decreased in magnitude with decreasing pH, and then it changed sign at low pH to reach a μ value of $\sim 0.5 \times 10^{-8}$ m^2 V^{-1} s^{-1} at a pH of ~3. The obtained IEP for MS2 was estimated at 3.5. Redman et al. (17) analyzed the electrophoretic mobility of MS2 under the same conditions and obtained identical results. In the current work, mobility was measured at three $NaNO_3$ solution concentrations (1 mM, 10 mM, and 100 mM) in the pH range of 2.5 to 7 (Fig. 3). For the 10 mM concentration at pH 7, the mobility (μ) value of $\sim -2 \times 10^{-8}$ m^2 V^{-1} s^{-1} is much lower than that obtained by Penrod et al. (14) and Redman et al. (17) under similar conditions, whereas results at a pH of 2.5 (μ value of $\sim 0.5 \times 10^{-8}$ m^2 V^{-1} s^{-1}) are similar. There is no obvious explanation for this difference. It may be linked to the preparation and purification of phage suspension. We avoided the use of CsCl gradient purification, which has been shown to favor virus aggregation in some instances. This aggregation is known to strongly impact electrokinetics (10). Zolotukhin et al. (28) showed that treatment with CsCl leads to a reduction of viral infectivity in recombinant adeno-associated virus as a result of probable particle aggregation. Hosokawa et al. (6) also demonstrated that the standard method of ultracentrifugation in CsCl for preparing a high titer of purified recombinant ade-

Downloaded from https://journals.asm.org/journal/aem on 18 December 2024 by 72.80.70.191.

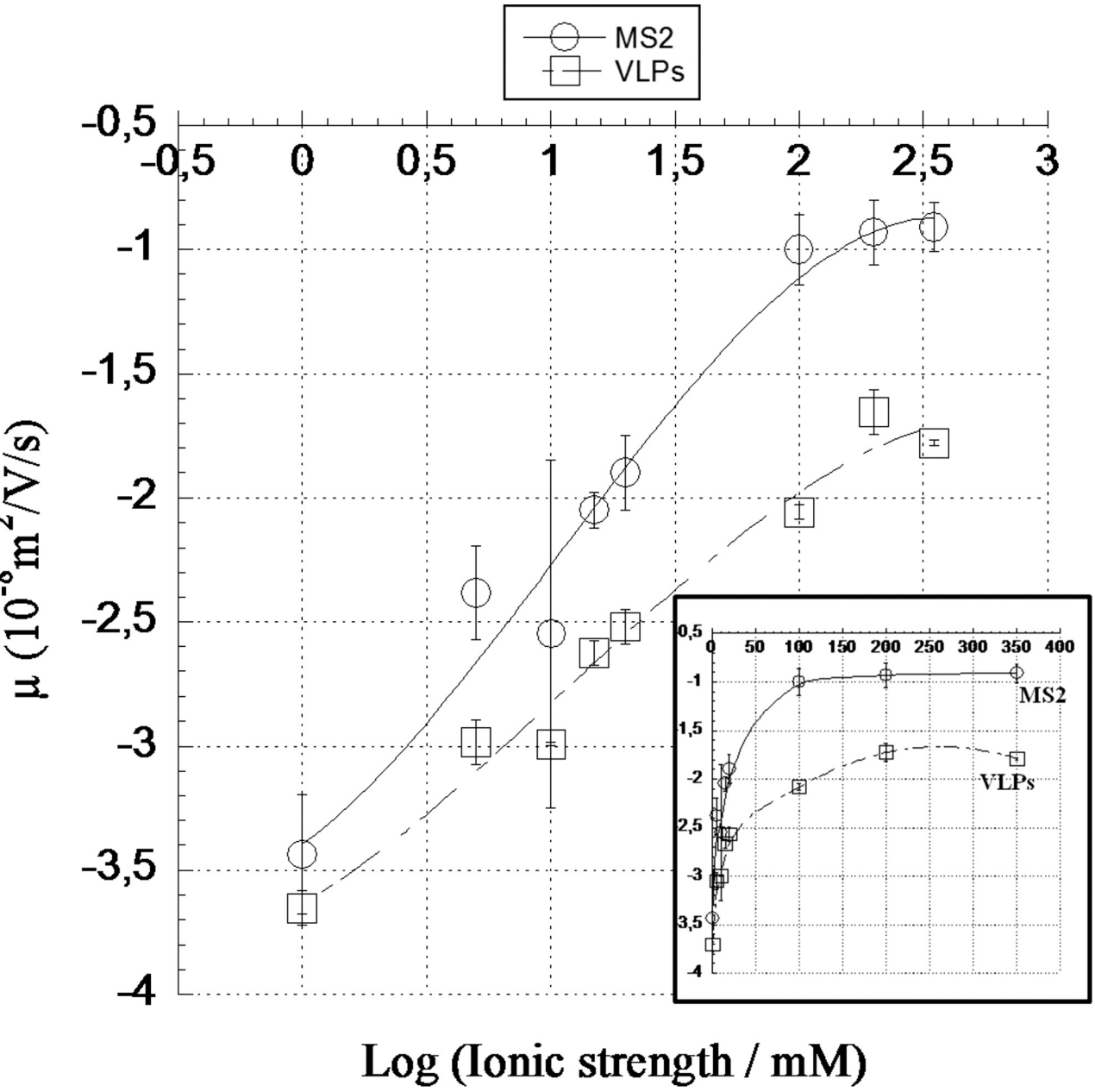

FIG. 4. Electrophoretic mobilities of MS2 bacteriophage and MS2 VLPs as a function of log of ionic strength at pH 7. The solid and dotted lines are only guides to the eye. (Inset) Electrophoretic mobilities of MS2 bacteriophage and MS2 VLPs as a function of ionic strength (linear scale) at pH 7. Error bars indicate standard deviations.

novirus leads to a complete loss of adenovirus activity, again possibly connected to virus aggregation. Finally, as proof of the importance that should be given to the preparation procedure of the viral suspension, Wright et al. (26) evidenced that adeno-associated virus vectors purified by double CsCl gradient ultracentrifugation are systematically aggregated at low ionic strengths. This clearly highlights that any comparison between electrokinetics of different viral particles is relevant provided that measurements are carried out under identical conditions (e.g., nature of electrolyte) and on isolated viral particles using similar purification protocols. These important elements were taken into consideration here for an appropriate analysis of electrokinetics of MS2 and corresponding VLPs. Size measurements and electron microscopy revealed that, under conditions where aggregation is absent (pH $>$ 4) (Fig. 2), the sizes of MS2 VLPs are similar to those of complete viruses. However, the inner part of VLPs appears less electron dense, supporting the idea that VLPs lack the inner viral RNA component.

Electrophoretic mobility. Upon sole consideration of IEP values obtained for MS2 and MS2 VLPs (3.5 to 3.9), one could conclude that surface properties of viruses are governed solely by the more external amino acid residues of the capsid (15). However, this hypothesis does not support either the evolution of the electrokinetic profile as a function of the ionic strength

Downloaded from https://journals.asm.org/journal/aem on 18 December 2024 by 72.80.70.191.

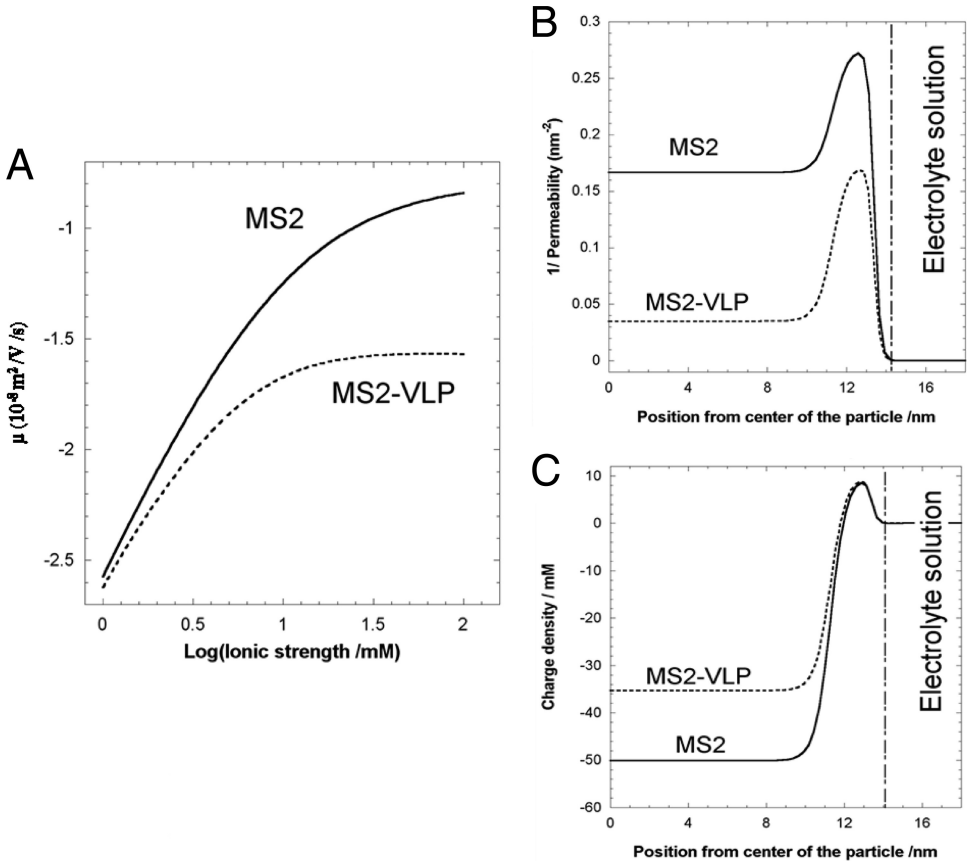

FIG. 5. (A) Qualitative reconstruction of the respective positioning of the mobility versus ionic strength curves for MS2 and MS2 VLPs. This figure illustrates the electrostatic and hydrodynamic impacts of the inner part of viral particles on the electrophoretic mobility (μ). The data were obtained using the theory detailed in reference 10 for the electrohydrodynamics of soft multilayered particles. The spatial profiles for the friction ($\sim$1/permeability) and charge density (expressed in concentration of equivalently ionized groups) across the particles are detailed in panels B and C, respectively. As a basis for these calculations, we considered for the heterogeneity parameters (quantities α in reference 10) and for the inner RNA and capsid thicknesses the values detailed in reference 10 for MS2 phage.

(presence of a plateau in mobility, typical of a significant particle permeability) (4, 10) or the aggregation profiles of the virus, which also clearly reflect the behavior of a soft multilayered particle, as detailed below. In line with the theory and experiments reported by Langlet et al. (10), the IEP value of $\sim$3.5 for MS2 is typical for the high permeability of this virus to electroosmotic flow. The pH values defining zero charge density for the inner RNA part of the virus and the capsid shell are about 2.9 and 9, respectively. If MS2 phage were sensu stricto impermeable to external flow, then electrokinetics would reflect the dissociation properties solely of the amino acids within the capsid, with a resulting IEP of about 9. This hypothesis is, however, not correct, in view of the IEP of $\sim$3.5 obtained for MS2. For hard (impermeable) particles, electroosmotic flow field lines follow the contour of the particle, while for soft particles, like viruses, which exhibit a certain degree of permeability, those flow field lines penetrate within the particle. The IEP of 3.5 indicates that electrokinetics is able to probe charge properties (i.e., nature, distribution, and dissociation) of the inner RNA component of the MS2 phage, in line with the marked mobility plateau reached at large ionic strengths. In theory, the pH values that neutralize the density of charges carried by the inner RNA and outer capsid are 2.9 and 9, respectively (10). Then, the proteic capsid of MS2 carries at a pH of 7 a positive net charge, while the inner RNA is negatively charged under such a pH condition. With the assumption that VLPs are entirely devoid of any RNA constituent, the mobility for these particles would be positive over the range of ionic strengths examined in this study. Our results obviously indicate that this scenario is not possible and thereby support the presence of some internal negatively charged component at pH 7 for the MS2 VLPs, possibly associated with the presence of host-derived RNAs but also with proteins or other materials from host bacteria where VLPs are assembled. This internal component is significantly probed by the flow in electrophoresis experiments, which explains the low IEP value observed for the VLPs and the presence of a plateau in mobility at large ionic strengths. A question then arises about the nature of the inner material of MS2 VLPs. By nature, this cannot be viral RNA. However, bacterial components, including bacterial RNA, could fill, at least partially, the "empty" inner space of the VLPs, as demonstrated by Pickett and Peabody (16).

Because from the literature much information is known about the structure of MS2 and about the nature, quantity, and radial distribution of the charges it carries, theoretical compu-

Downloaded from https://journals.asm.org/journal/aem on 18 December 2024 by 72.80.70.191.

tation of MS2 mobility as a function of pH can be performed using an advanced electrohydrodynamic model for isolated (i.e., not aggregated) multilayered particles, as detailed in reference 10. The nonlinear Poisson Boltzmann and Brinkman equations considered in the formalism detailed previously (10) allow for the computation of the spatial distributions of electrostatic and hydrodynamic fields all across the virus, as well as the distribution profiles of ions from the center of the virus to the bulk electrolyte solution. The effect of the externally applied electric field (electrophoresis) on the distributions of these key physical quantities is explicitly taken into account. Evaluation of particle electrophoretic mobility is then possible from the asymptotic behavior of the electroosmotic flow field at infinite distances from the virus. In particular, Langlet et al. (10) demonstrated that electrophoretic mobility data for MS2 could be very well reproduced by this theory in the pH range where aggregation is absent ($pH > 4$) but that important discrepancies appeared at lower pH ($pH < 4$). The modeling largely overestimates the magnitude of the mobility in the pH range where there is aggregation. It further highlights that an "S-type" dependence on pH is expected for the mobility (μ) of isolated viruses, with a clearly defined change in sign of mobility at low pH, similarly to that observed in the case of VLPs.

Quantitative evaluation of the electrokinetic response of VLPs using detailed data describing VLP chemical composition is currently impossible due to the lack of knowledge on the inner-material quantity, nature, and charge repartition for this type of particle. Despite this limitation, the comparison between the theoretical and experimental dependencies of μ on pH as obtained for MS2 (10) qualitatively corroborates that the behavior of μ at low pH for VLPs is in agreement with that typically expected for isolated viral particles containing a negatively charged inner component surrounded by a proteinaceous shell. The absence of aggregation for VLPs at low pH is further independently confirmed here by size measurements.

Let us now comment on the respective densities of the inner negatively charged components carried by MS2 VLPs and MS2 phage and discuss how any underlying differences could be reflected in the profiles of mobility versus salt concentration. In their analysis of electrokinetics of soft multilayered particles, Langlet et al. (10) evaluated the effect of internal charge density of MS2 phage on the concentration dependence of mobility, while maintaining constant the charge density within the most external layer of the particle and the typical flow penetration. For particles with a significant flow penetration compared to the thickness of the external layer (in the case of MS2 phage [10]), results show that increasing the magnitude of the inner charge density of the particle results in a stronger increase (in magnitude) of the mobility with decreasing electrolyte concentrations from 100 mM to 1 mM. In other words, the slope of the curve μ versus logarithm of the salt concentration is most important for permeable multilayered particles characterized by a high density of charges in their inner part. This trend agrees with data shown in Fig. 4 where the dependence on ionic strength for the mobility (μ) of MS2 VLPs lacking inner RNA is less pronounced than that observed for MS2 phage. The results shown in Fig. 4 further demonstrate that the μ values measured for MS2 and VLPs in the plateau regime significantly differ. A possible reason for such a difference is the effect of the inner material of the particle on the overall permeability properties. Since the internal part of VLPs is not as dense as that for MS2 phage, the hydrodynamic resistance offered by the inner particle component is expected to be more significant in the case of MS2, thereby reducing MS2 mobility (in magnitude) compared to that of VLPs, which is in line with data shown in Fig. 4. In addition, the absence of maturase protein in VLPs may lead, together with the "empty character" of these particles, to a proteic capsid that is more porous and less structured (or less compact) than that of MS2, where maturase protein and/or internal RNA contributes to conferring a certain integrity or compactness to the capsid. As a result, flow penetration within VLPs would be greater than that within complete MS2 phage.

The previously discussed electrostatic and hydrodynamic impacts of internal-material content on the electrophoretic mobility of MS2 and MS2 VLPs are illustrated in Fig. 5. The figure shows electrokinetic profiles computed from the theory of Langlet et al. (10) for a particle with distinct internal and external components, with variations in the internal charge density and/or the overall particle permeability. The thickness of the constituting layers as well as the sign of the inner and outer charge densities is chosen to approach the case of complete MS2 phage under the condition of a pH of 7. From the data shown in Fig. 5, we conclude that a concomitant decrease in the inner particle charge density and increase in particle permeability qualitatively reproduce the respective positioning of the mobility versus salt concentration profiles measured for MS2 VLPs and complete MS2 phage. We emphasize that it is not possible to quantify the difference between the density of internal host material for VLPs and that of RNA for MS2 because so far there are no detailed data on the conformation of the VLP coat protein and the chemical composition of the inner host material of VLPs.

Aggregation. The data shown in Fig. 2 underline that the stability properties of VLP suspensions against aggregation not only differ from those obtained for MS2 suspensions but also do not follow the classical picture expected from conventional DLVO theory for colloidal stability. According to the latter, it is predicted that upon increase of ionic strength, the compression of the electric double layer developed around the interacting particles leads to a significant decrease and/or suppression of the repulsive electrostatic forces between neighboring particles, thereby favoring their aggregation. Additionally, it is expected from this theory that attractive interactions (e.g., Van der Waals) are systematically dominant for particles carrying a zero net charge, thus leading to instability. In case of MS2 VLPs, however, we observe that aggregates are formed at a pH about equal to the IEP for sufficiently low ionic strength (below 10 mM) and that particles remain in isolated form at 100 mM salt concentration irrespective of the pH value. To explain the high stability of VLPs in 100 mM $NaNO_3$ over the pH range from 2.5 to 7 compared to that of MS2, we may argue that the presence/absence of maturase in MS2/VLPs, respectively, modifies the steric contribution of the overall interaction between the particles, thus leading to different stability properties, as hypothesized by da Silva et al. (2) in their analysis of norovirus GI and GII VLP stability. However, recalling that steric repulsions are of shorter range than electrostatic interactions (especially at low ionic strengths), one should also measure a remarkable stability of the VLPs at low ionic strengths in the pH range from 2.5 to 7, where large-range repulsive inter-

Sarepta Exhibit 1035, page 8

Downloaded from https://journals.asm.org/journal/aem on 18 December 2024 by 72.80.70.191.

actions exist in addition to the aforementioned steric contribution. This is not observed for VLPs that are destabilized for some critical pH value near the IEP. Invoking steric interactions cannot be sufficient to explain the variation in stability of VLPs with varying ionic strengths and pH values. In the analysis by da Silva et al. (2) on the adsorption/aggregation properties of norovirus GI and GII VLPs, the extreme stability of those particles at high ionic strength, similar to that obtained here for MS2 VLPs, "may be unique to VLPs, where the lack of RNA could change particle stability." This hypothesis by da Silva et al. (2) is exactly the one we support as described below from interpretation of MS2 and VLP size measurements.

To qualitatively understand the peculiar and *a priori* "abnormal" stability behavior of VLPs at 100 mM, we reason in terms of the theory recently developed by Duval et al. (5) for predicting the magnitude of electrostatic interactions between particles that consist of concentric layers carrying functional groups with different dissociation properties. Duval et al. (5) demonstrated that the sign and magnitude of the electrostatic interactions between multilayered particles are basically determined by the charge properties of the layers located within a depth of the order of the Debye length κ^{-1}. This distance reflects the typical distance for electrostatic interactions between particles or equivalently the characteristic extension of the electric double layer around/within the particle (see, for instance, references 4 and 5 for expression of κ^{-1} versus salt concentration). For viruses which consist of an inner RNA component of radius δ_1 of ~11.3 nm and an outer capsid shell of thickness δ_2 of ~2.1 nm (10), the contribution of the internal RNA component in determining the repulsive electrostatic interactions between neighboring viruses is therefore governed by the dimensionless number $\kappa\delta_2$. The electrostatic interactions between VLPs should then be strictly governed by the nature and the dissociation properties of the functional groups located within the capsid shell under the condition $\kappa\delta_2 \gg 1$, which is met at sufficiently high salt concentration. Under the other limiting condition, where $\kappa\delta_2 \ll 1$, electrostatic interactions are determined mainly by the details of nature/distribution of charges within the internal particle component. For intermediate conditions, the electrostatic interactions depend on the charge properties of both the capsid and the inner part of the virus. For 100 mM, 10 mM, and 1 mM salt concentration conditions, we find $\kappa\delta_2$ values of ~2.2, 0.7, and 0.2, respectively. Accordingly, at 100 mM, the capsid thickness is significantly above the typical Debye length κ^{-1}, and it is then the capsid region of the VLPs that significantly determines their electrostatic interactions. As a result, we expect that repulsive interactions between VLPs systematically take place for a pH of <9, i.e., the pH range where the capsid shell is positively charged.

In the pH range of 2.5 to 7 investigated in this study, the net charge carried by the capsid never reaches a zero value, so that the electrostatic interactions between VLPs cannot be rigorously cancelled in this pH range. From stability data at 100 mM (Fig. 2), we infer that the finite magnitude of the repulsive electrostatic forces between VLPs in the pH range of 2.5 to 7 is always sufficient to counterbalance the short-range attractive forces and thus prevent aggregation in this pH range. With lowering electrolyte concentration, $\kappa\delta_2$ significantly decreases, and therefore the contribution of the inner material of VLPs in governing the overall electrostatic interactions gradually becomes predominant. The pH value marking the zero condition for internal charge of VLPs is necessarily much lower than that for the capsid, as argued from the IEP measured for VLPs. Denoting as pH_c this critical pH value, one expects from the theory of Duval et al. (5) that for a $\kappa\delta_2$ value of $\ll 1$ and pH values below and above pH_c, where the inner material is positively and negatively charged, respectively, VLPs experience significant repulsive electrostatic interactions, thereby favoring stability of VLP suspensions against aggregation. These arguments qualitatively support the data of Fig. 2, which show that VLPs in 1 mM and 10 mM salt concentration are in isolated form for pH above and below a critical pH whose value is in the range from 3 to 4. This discussion, though qualitative, has the merit to provide a comprehensive explanation for the *a priori* anomalous stability properties of VLPs with varying pH values and salt concentrations. The recent theory on electrostatic interactions between multilayered particles (5) provides the physical basis for understanding these properties. At the current stage of our comprehension of the composition, spatial distribution, and dissociation of the charges located in the internal and capsid parts of VLPs, a complete quantitative theoretical evaluation of the stability diagrams for VLPs is unfortunately not possible.

The stability properties of MS2 phage are similar to those for VLPs at high pH, but important discrepancies arise at low pH (pH < IEP). In line with data given by Langlet et al. (10), the aggregation profiles obtained for MS2 phage are furthermore completely independent of the electrolyte concentration. This strongly suggests that interactions other than electrostatic interactions predominantly govern the stability properties of MS2, particularly at a pH that is lower than the IEP. By comparing the stability profiles of MS2 and VLPs for pH values lower than 4, we hypothesize that the presence of genome material within MS2 phage considerably increases its hydrophobic character. In other words, the presence of the viral genome could be, by its very interaction with the capsomers, responsible for particular conformations of the protein on the capsid that are not met for VLPs. In turn, the contribution of the attractive interaction forces would be more important for MS2 than for VLPs and would systematically result in particle aggregation at low pH values. It is also possible that variations in conformation/composition of the proteins constituting the capsid of VLPs and MS2 phage are not rigorously identical and lead to different stability features at low pH following variations in hydrophobicity and/or Hamaker constant. This argument is supported by two facts. First, the capsid of MS2 phage consists of 180 copies of capsid proteins and a single copy of a maturation protein, whereas the capsid of VLPs lacks the maturation protein, and second, this maturation protein is known to impact significantly the three-dimensional structure of the viral capsid (8). However, reasoning on the sole basis of the outer capsid (of MS2 or VLPs) cannot be sufficient because it does not explain the presence of a mobility plateau value at large ionic strengths. In addition, because MS2 contains only one copy of the maturase protein, compared to 180 copies of the major capsid protein, the absence of this single maturase in the VLP capsid is not likely to lead to significant electrostatic changes and thus differences in electrokinetic and stability properties between the two types of particles. Despite this uncertainty in the origin of stability differences between MS2 and VLPs at low pH, all results reported in this work clearly show some limitations in the use of VLPs as model systems for predicting virus behavior.

Sarepta Exhibit 1035, page 9

Downloaded from https://journals.asm.org/journal/aem on 18 December 2024 by 72.80.70.191.

ACKNOWLEDGMENTS

This work was supported by program grant ANR-07-PNRA-008 (ADHERESIST) from the ANR (Agence Nationale de la Recherche).

D. S. Peabody (University of New Mexico) is acknowledged for providing the pETCT plasmid for the MS2 VLP synthesis.

REFERENCES

1. **Association Francaise de Normalisation.** 2001. NF EN ISO 10705-1. Water quality. Detection and enumeration of F-specific RNA bacteriophages. Association Française de Normalisation, La Plaine Saint-Denis, France.
1a. **Ausar, S. F., T. R. Foubert, M. H. Hudson, T. S. Vedvick, and C. R. Middaugh.** 2006. Conformational stability and disassembly of Norwalk virus-like particles. Effect of pH and temperature. J. Biol. Chem. **281:**19478–19488.
2. **da Silva, A. K., O. V. Kavanagh, M. K. Estes, and M. Elimelech.** 2011. Adsorption and aggregation properties of norovirus GI and GII virus-like particles demonstrate differing responses to solution chemistry. Environ. Sci. Technol. **45:**520–526.
3. **Duval, J. F. L., and F. Gaboriaud.** 2010. Progress in electrohydrodynamics of soft microbial particle interphases. Curr. Opin. Colloid Interface Sci. **15:**184–195.
4. **Duval, J. F. L., and H. Ohshima.** 2006. Electrophoresis of diffuse soft particles. Langmuir **22:**3533–3546.
5. **Duval, J. F. L., J. Merlin, and P. A. L. Narayana.** 2011. Electrostatic interactions between diffuse soft multi-layered (bio)particles: beyond Debye-Huckel approximation and Deryagin formulation. Phys. Chem. Chem. Phys. **13:**1037–1053.
6. **Hosokawa, M., et al.** 2002. Preparation of purified, sterilized, and stable adenovirus vectors using albumin. J. Virol. Methods **103:**191–199.
7. **Jiang, X., M. Wang, D. Y. Graham, and M. K. Estes.** 1992. Expression, self-assembly, and antigenicity of the Norwalk virus capsid protein. J. Virol. **66:**6527–6532.
8. **Kuzmanovic, D. A., I. Elashvili, C. Wick, C. O'Connell, and S. Krueger.** 2006.The MS2 coat protein shell is likely assembled under tension: a novel role for the MS2 bacteriophage A protein as revealed by small-angle neutron scattering. J. Mol. Biol. **355:**1095–1111.
9. **Langlet, J., F. Gaboriaud, J. F. L. Duval, and C. Gantzer.** 2008. Aggregation and surface properties of F-specific RNA phages: implication for membrane filtration processes. Water Res. **42:**2769–2777.
10. **Langlet, J., F. Gaboriaud, C. Gantzer, and J. F. L. Duval.** 2008. Impact of chemical and structural anisotropy on the electrophoretic mobility of spherical soft multilayer particles: the case of bacteriophage MS2. Biophys. J. **94:**3293–3312.
11. **Langlet, J., et al.** 2009. Efficiency of MS2 phage and Qbeta phage removal by membrane filtration in water treatment: applicability of real-time RT-PCR method. J. Membr. Sci. **326:**111–116.
12. **Lima, S. M., et al.** 2006. Dissecting the role of protein-protein and protein-nucleic acid interactions in MS2 bacteriophage stability. FEBS J. **273:**1463–1475.
13. **Loisy, F., R. L. Atmar, J. Cohen, A. Bosch, and F. Le Guyader.** 2004. Rotavirus VLP2/6: a new tool to track rotavirus in the marine environment. Res. Microbiol. **155:**575–578.
14. **Penrod, S. L., T. M. Olson, and S. B. Grant.** 1995. Whole particle microelectrophoresis for small viruses. J. Colloid Interface Sci. **173:**521–523.
15. **Penrod, S. L., T. M. Olson, and S. B. Grant.** 1996. Deposition kinetics of two viruses in packed beds of quartz granular media. Langmuir **12:**5576–5587.
16. **Pickett, G. G., and D. S. Peabody.** 1993. Encapsidation of heterologous RNAs by bacteriophage MS2 coat protein. Nucleic Acids Res. **21:**4621–4626.
17. **Redman, J. A., S. B. Grant, T. M. Olson, M. E. Hardy, and M. K. Estes.** 1997. Filtration of recombinant Norwalk virus particles and bacteriophage MS2 in quartz sand: importance of electrostatic interactions. Environ. Sci. Technol. **31:**3378–3383.
18. **Sambrook, J., and D. W. Russell.** 2001. Molecular cloning: a laboratory manual, vol. 1, p. I.24–I.29. Cold Spring Harbor Laboratory Press, Cold Spring Harbor, NY.
19. **Schaldach, C. M., W. L. Bourcier, H. F. Shaw, B. E. Viani, and W. D. Wilson.** 2006. The influence of ionic strength on the interaction of viruses with charged surfaces under environmental conditions. J. Colloid Interface Sci. **294:**1–10.
20. **Schijven, J. F., and M. Hassanizadeh.** 2000. Removal of viruses by soil passage: overview of modeling, processes, and parameters. Crit. Rev. Environ. Sci. Technol. **30:**49–127.
21. **Shirasaki, N., T. Matsushita, Y. Matsui, A. Oshiba, and K. Ohno.** 2010. Estimation of norovirus removal performance in a coagulation-rapid sand filtration process by using recombinant norovirus VLPs. Water Res. **44:** 1307–1316.
22. **Valegård, K., L. Liljas, K. Fridborg, and T. Unge.** 1990. The three-dimensional structure of the bacterial virus MS2. Nature **345:**36–41.
23. **Valegård, K., L. Liljas, K. Fridborg, and T. Unge.** 1991. Structure determination of the bacteriophage MS2. Acta Crystallogr. B Struct. Sci. **47:**949–960.
24. **Valegård, K., K. Fridborg, and L. Liljas.** 1994. Crystallization and preliminary X-ray diffraction studies of the bacteriophage Qbeta. Acta Crystallogr. D Biol. Crystallogr. **50:**105–109.
25. **van Voorthuizen, E. M., N. J. Ashbolt, and A. I. Schafer.** 2001. Role of hydrophobic and electrostatic interactions for initial enteric virus retention by MF membranes. J. Membr. Sci. **194:**69–79.
26. **Wright, J. F., et al.** 2005. Identification of factors that contribute to recombinant AAV2 particle and methods to prevent its occurrence during vector purification and formulation. Mol. Ther. **12:**171–178.
27. **Zerda, K. S., C. P. Gerba, K. C. Hou, and S. M. Goyal.** 1985. Adsorption of viruses to charge-modified silica. Appl. Environ. Microbiol. **49:**91–95.
28. **Zolotukhin, S., et al.** 1999. Recombinant adeno-associated virus purification using novel methods improves infectious titer and yield. Gene Ther. **6:**973–985.

Downloaded from https://journals.asm.org/journal/aem on 18 December 2024 by 72.80.70.191.